Effect of Local Binding on Stochastic Transport in Ion Channels

I. Kh. Kaufman*, W. A. T. Gibby*, D. G. Luchinsky*†, P. V. E. McClintock*,
*Department of Physics, Lancaster University, Lancaster LA1 4YB, UK
Email: p.v.e.mcclintock@lancaster.ac.uk
†SGT Inc., Greenbelt MD, 20770, USA

***Abstract*—Ionic Coulomb blockade (ICB) is an electrostatic phenomenon recently discovered in low-capacitance ion channels/nanopores. Depending on the fixed charge that is present, ICB strongly and selectively influences the ease with which a given type of ion can permeate the pore. The phenomenon arises from the discreteness of the charge-carriers, the dielectric self-energy, an electrostatic exclusion principle, and sequential pore neutralization, and it manifests itself strongly for divalent ions (e.g. Ca^{2+}). Ionic Coulomb blockade is closely analogous to electronic Coulomb blockade in quantum dots. In addition to the non-local 1D Coulomb interaction considered in the standard Coulomb blockade approach, we now propose a correction to take account of the singular part of the attraction to the binding site (i.e. local site binding). We show that this correction leads to a geometry-dependent shift of one of the barrierless resonant conduction points M_0^{CB}. We also show that local ion-ion repulsion accounts for a splitting of Ca^{2+} profiles observed earlier in Brownian dynamics simulations.**

I. Introduction

Ion channels provide for the selective transport of physiologically important ions (e.g. Na^+, K^+ and Ca^{2+}) through the bilipid membranes of biological cells. The channels consist of nanopores through proteins embedded in the membrane. Their selectivity for particular ions is determined by the electrostatically-driven stochastic motion of ions within a short, narrow selectivity filter (SF) carrying a binding site with fixed negative charge Q_f.

The permeation of ions through the pore is governed by ionic Coulomb blockade (ICB), a phenomenon that manifests itself in low-capacitance systems. It arises as a consequence of the discreteness of the charge-carriers, the dielectric self-energy U_s, an electrostatic exclusion principle, and sequential pore neutralisation as additional ions enter the pore [1]–[3]. ICB manifests itself strongly for divalent ions (e.g. Ca^{2+}) [2]. ICB is closely similar to its electronic counterpart in quantum dots [4].

The basic ICB description of the permeation and selectivity of ion channels has already been presented [3]. Here we extend this basic model by the introduction of corrections to allow for the singular part of the attraction of ions to the binding site (i.e. local site binding), in addition to the non-local 1D Coulomb interaction considered in the standard ICB approach [2]. We will find that the geometry-dependent shift of the ICB calcium resonant point M_0^{CB} resulting from this correction leads to a changed threshold IC_{50} for divalent blockade. We will also show that the presence of local (singular) ion-ion repulsion is what leads to the splitting of the Ca^{2+} probability density seen earlier in Brownian dynamics simulations [5], [6].

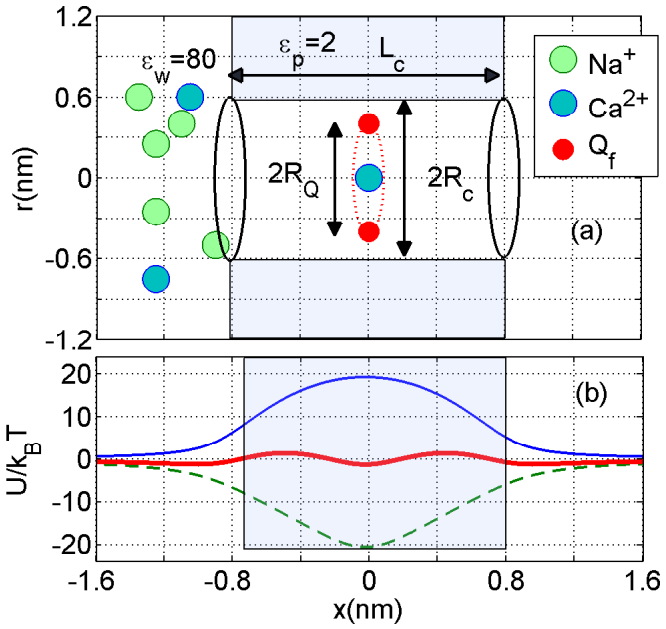

Fig. 1. (Modified from [3]) Extended electrostatic model of the selectivity filter of Ca^{2+} or Na^+ channel. (a) The model represents a channel as a negatively-charged, axisymmetric, water-filled, cylindrical pore of radius $R_c = 0.3-0.5$nm and length $L_c = 1.2-1.6$nm through the protein hub in the cellular membrane. The x-axis is coincident with the channel axis and $x = 0$ in the center of channel. There is a uniformly-charged, rigid ring of negative charge $|Q_f| = 0-8$ of radius R_Q. Ions move in single file along the channel axis. (b) Energetics of moving Ca^{2+} ion for fixed charge $Q_f = -1e$ (by Brownian dynamics simulations). The dielectric self-energy barrier U_q^{SE} (full blue line) is balanced by the site attraction U_{qQ}^{CB} (dashed green line) resulting in an almost barrier-less energy profile U_b (red solid line). See text for details.

In what follows we use dimensionless Gaussian units assuming the proton charge $e = 1$, $4\pi\varepsilon_0 = 1$ and $k_BT = 1$, where ε_0 is the permittivity of free space, k_B is Boltzmann's constant and T is the temperature.

II. Extended Electrostatic Model of Ion Channel

Fig. 1(a) shows the extended electrostatic model of the SF of a calcium/sodium ion channel, We represent it as a negatively-charged, axisymmetric, water-filled, cylindrical pore of radius $R_c = 0.3-0.5$nm and length $L_c = 1.2-1.6$nm through the protein hub in the cellular membrane The x-axis is coincident

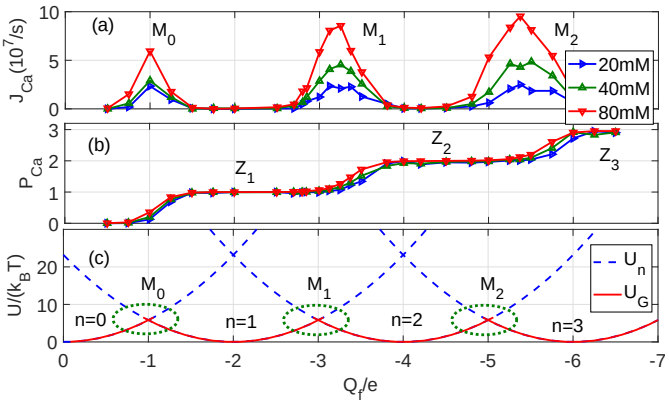

Fig. 2. (Reworked from [3]) Brownian dynamics simulations of multi-ion conduction and occupancy in a Ca^{2+} channel model *vs* the effective fixed charge Q_f. (a) Conduction bands in the Ca^{2+} current J for pure Ca^{2+} baths of different concentration (20, 40 and 80mM as indicated). (b) Coulomb staircase for the occupancy P. (c) The excess self-energy U_n and ground state energy U_G *vs* Q_f for channels containing $n = 0, 1, 2$ and 3 Ca^{2+} ions. The conduction bands M_n and the blockade/neutralisation points Z_n are discussed in the text.

with the channel axis and $x = 0$ in the center of channel. There is a symmetrically-placed, uniformly-charged, rigid ring of negative charge $|Q_f| = 0-8$. Extending the earlier model, the radius of this charged ring R_Q could be different from the channel radius R_c, corresponding to the charged residues moving partially into the channel. We take both the water and the protein to be homogeneous continua with dielectric constants $\varepsilon_w = 80$ and $\varepsilon_p = 2$, respectively.

Fig. 1(b) illustrates the phenomenon of resonant barrier-less conduction, which is typical of electrostatic models and which occurs when the energy of ion-site attraction U_{gQ} balances the dielectric self-energy barrier U_q^{SE} [2], [7], [8].

This generic electrostatic channel model is similar to that used previously [5], [9]–[11]. Details of the model, and its validity and limitations, have already been discussed [6].

III. Ionic Coulomb blockade

We consider the stochastic transport of a fully-hydrated ion of charge $q = ze$ through the above model channel, focusing on the divalent case ($z = 2$).

Fig. (2)(a) illustrates the multi-ion Ca^{2+} conduction bands and (b) shows the corresponding Coulomb staircase in occupancy, as revealed by Brownian dynamics simulations. The ground state energy diagram for such conductance is plotted in (c). The ICB model [3] states that resonant (barrier-less) conduction points M_n occur when the difference in free energy ΔG_n between states s_{n+1} (with $n+1$ ions near the center of the SF) and s_n (channel with n ions in the SF plus 1 ion in the bulk) is zero:

$$\Delta G_n = G_{n+1} - G_n = U_{n+1} - U_n - T\Delta S_n \qquad (1)$$

where G_i refers to state s_i, U_n is the potential energy and ΔS_n is the entropy difference. When $\partial U_n/\partial Q_f = 0$, there are stable ICB points Z_n.

The standard ICB model assumes that U_n with $\{n\}$ similar ions near the centre is equal to the dielectric self-energy U_n^{SE} of the excess (or total) charge of the SF Q_n:

$$Q_n = nq + Q_f; \quad U_n = U_n^{SE} = \frac{Q_n^2}{2C_s} \qquad (2)$$

$$C_s = \frac{R_c^2}{\lambda_B L_c}; \quad \lambda_B = \frac{e^2}{\varepsilon_w k_B T} \qquad (3)$$

where C_s is the SF self-capacity and λ_B is the Bjerrum length (for water $\lambda_B = 0.7$nm) [10].

For simplicity, we consider the first resonant point M_0 [6] corresponding to the movement of a single ion through an otherwise empty SF (the $s_0 \to s_1 \to s_0$ transition) so we temporarily ignore the ion-ion interaction term U_{qq}. Expanding the quadratic form in (3) gives us the following decomposition (for $n = 1$)

$$U_1 = U_q^{SE} + U_Q^{SE} + U_{qQ}^{CB} \qquad (4)$$

$$U_q^{SE} = \frac{q^2}{2C_s}; \quad U_Q^{SE} = \frac{Q_f^2}{2C_s}; \quad U_{qQ}^{CB} = \frac{qQ_f}{C_s};$$

where U_q^{SE} and U_Q^{SE} are respectively the ion and fixed charge self-energies, and U_{qQ}^{CB} is the 1D Coulomb ion-site attraction energy [10], [12].

The base position (without the entropy term) for resonant conduction is defined by the condition forbarrier-less motion $\Delta U_n = U_{n+1} - U_n = 0$

$$U_{qQ}^{CB} = 0; \Rightarrow M_0^{CB} = -q/2 \quad Z_1 = -q \qquad (5)$$

whereas Z_n corresponds to the $Q_n = 0$ SF neutralisation condition. Inclusion of the entropy term $T\Delta S$ leads to a concentration-related shift of the resonance point:

$$M_0^{TS} = M_0^{CB} + \delta M_0^{TS}; \quad \delta M_0^{TS} = \log(\frac{n_b}{n_0}) \qquad (6)$$

where n_b is the number density of selected ions in the bulk, $n_0 = 1/V_{SF}$ is the reference density, and $V_{SF} = \pi R_c^2 L_c$ is the volume of the SF; note that $\delta M_0 = 0$ for $n_b = n_0$. The reference concentration c_0 for a typical SF geometry corresponds to $c_0 \approx$200mM/l. The dependence of the resonance point's position on V_{SF} coincides with both simulations and with earlier analytic results [13], [14].

IV. Local binding

Next we introduce a local binding correction by adding the direct but ε-screened Coulomb $q \Leftrightarrow Q_f$ interaction [15] with energy U_{qQ}^{LB} to the total energy balance It leads to a geometry-dependent shift in the resonance point M_0^{LB} [2], [16] :

$$U_1 = U_1^{CB} + \delta U_{qQ}^{LB}; \quad U_{qQ}^{LB} = \frac{qQ_f\lambda_B}{\delta R_Q}; \qquad (7)$$

$$M_0^{LB} = M_0^{CB}\frac{\beta_Q}{\beta_Q + \beta_c} \qquad (8)$$

where R_Q is the radius of the charged ring at the binding site and we introduce two dimensionless geometrical factors: the "charge offset ratio" $\beta_Q = R_Q/R_c$ and the "SF shape ratio"

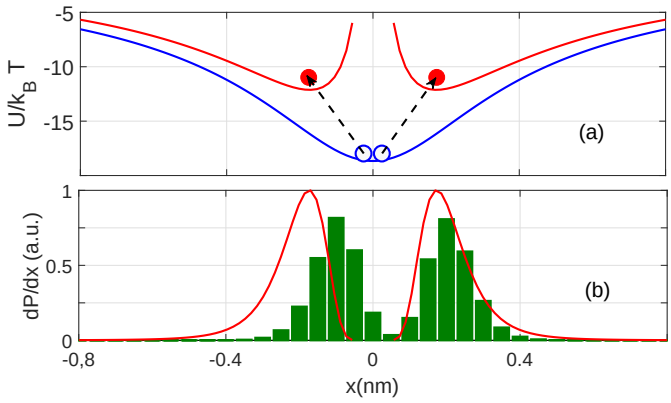

Fig. 3. Effect of local binding and local repulsion on the energy and occupancy profiles for Ca^{2+} ions inside the selectivity filter, in accordance with (13) for the Z_1 resonance point ($Q_f = 4$) and $R_Q = R_c$. (a) Energetics of ion-ion repulsion: local binding component U_{qQ}^{LB} (blue line, blue circles) and total energy taking account oflocal binding and repulsion U_q^{CB+LB}(red line, red circles for the split equilibrium positions). (b) The split calcium profile (green histogram) obtained by self-consistent Brownian dynamics simulation [16] is consistent with the analytic result (red solid line)

$\beta_c = R_c/L_c$. For an embedded charge ring ($R_Q = R_c, \beta_Q = 1$), equation (8) reduces to

$$M_0^{LB} = \frac{M_0^{CB}}{1+\beta_c} \approx M_0^{CB}(1-\beta_c) \tag{9}$$

For typical geometries ($R_c = R_Q$ =0.3nm , L_c = 1.5nm) the correction for local binding can be about 0.2. In summary,

$$M_0 = M_0^{CB} - M_0^{CB}\beta_c + \log\frac{n_b}{n_0}; \tag{10}$$

The "shift-equation" (10) allows us to describe the whole range of ICB phenomenona, as embodied in different shifts of M_0 and their possible interference such as a divalent blockade and its dependence on Q_f [2], [17], or concentration-related shifts of the Coulomb staircase –

- The standard ICB optimal conduction point M_0^{CB} defines the barrier-less point for ion of charge q with $\beta_c \to 0$ at the standard bulk density n_0.
- The local-binding shift δM_0^{LB} accounts for the real shape of the SF and/or for R_Q.
- The concentration-related shift δM_0^{TS} describes the influence of n_b.
- The occurrence of interference between δM_0^{LB} and δM_0^{TS} could explain observable differences in divalent blockade thresholds IC_{50} between equally-charged (D/E) mutants of the calcium [17] or bacterial sodium channels [18].

The axial potential energy profiles for the ICB model can be derived from the 1D Coulomb gas approximation [10], [12]:

$$U_q^{SE}(x) = U_q^{SE}\left(1-(2x/L_c)^2\right) \tag{11}$$
$$U_{qQ}^{CB}(x) = U_{qQ}^{CB}\left(1-(2|x|/L_c)\right) \tag{12}$$
$$U_{SF}^{CB} = U_q^{SE} + U_{qQ}^{CB} \tag{13}$$

where $U_q^{SE}(x)$ is the dielectric self-energy profile and $U_{qQ}^{CB}(x)$ is the ion-site binding energy.

Additional local binding corrections can be calculated from Coulomb's law [15]:

$$\delta U_{qQ}^{LB} = U_{qQ}^{LB}\left(1+(x/R_Q)^2\right)^{-1/2} \tag{14}$$
$$U_{qQ}^{LB} = U_{qQ}^{CB} + \delta U_{qQ}^{LB} \tag{15}$$
$$U_{SF}^{LB} = U_q^{SE} + U_{qQ}^{LB} \tag{16}$$

V. Local ion-ion repulsion

In the above analytics we ignored ion-ion repulsion, but here we take it explicitly into account and work out its consequences. For simplicity we consider 2 similar ions located symmetrically $(-x_q, +x_q)$ around Q_f at $x = 0$. In such a case, the 1D Coulomb ion-ion interaction $U_q q^{CB}$ and the additional local Coulomb repulsion $\delta U_q q^{LB}$ are respectively:

$$U_{qq}^{CB} = -\frac{q^2 4x_q\lambda_B}{R_c^2}; \quad \delta U_{qq}^{LR} = \frac{q^2\lambda_B}{2x_q}. \tag{17}$$

The total energy of an ion inside the SF, allowing for both local binding and local repulsion, can be expressed as:

$$U_{SF}^{LR} = U_{SF}^{LB} + \frac{1}{2}(U_{qq}^{CB} + \delta U_{qq}^{LR}) \tag{18}$$

Hence for the neutralization point Z_1 ($Q_n = 2q + Q = 0$), the profile is defined by local components only.

Fig. 3(a) shows that the energy function $U_q^{LR}(x)$ has two off-center minima x_{min} defining a splitting of the Ca^{2+} occupancy profile. Thus, by taking account of local binding and of the local ion-ion interaction in the SF, we arrive at an explicit, self-consistent, analytic explanation of the splitting of the multi-ion occupancy profiles observed earlier in Brownian dynamics simulations [5], [6], [16], in self-consistent numerical solutions of the Poisson equation [16], and in analytic calculations [19], [20] modelling non-self-consistent potentials.

This splitting leads to significant increases in ionic energy and eventually to knock-on escape. Note that the "binding points" ($\pm x_{min}$) are unconnected with any physical binding sites different from the main Q_f-related site. This situation can be described as dynamic site binding and/or self-organisation of ions inside the SF (see also [11], [21]).

Fig. 3(b) compares the Ca^{2+} occupancy profile $\rho(x)$ returned by BD simulations (green histogram) with that estimated from the potential energy profile $U(x)$ as $\rho(x) = \exp(-U(x))$ (red solid line). The satisfactory agreement obtained can be regarded as confirming the consistency of our model.

Fig. 4 shows the evolution of the Ca^{2+} profile with varying Q_f as found from BD simulations [16], [22]. Fig. 4(a) shows the simulated calcium occupancy P of the SF vs Q_f for one bath concentration, demonstrating the standard Coulomb staircase shape. The single-ion $Z_1 \approx 2e$ and double-ion $Z_2 \approx 4e$ neutralisation points are indicated. In (b) there is an (unsplit) single-ion occupancy profile for the Z_1 point, which appears due to ICB and local binding of the ion to Q_f. In (c) the local repulsion provides for self-organisation of the ions and splitting of the occupancy profile for the double-ion Z_2 point. Note that, for intermediate points (between Z_1 and Z_2), the profiles will be mixed, having one to three peeks.

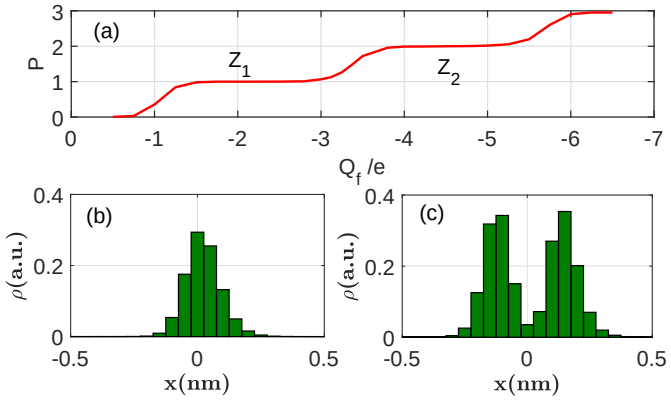

Fig. 4. Evolution of calcium profile *vs.* fixed charge Q_f from Brownian dynamics simulations [16]. (a) Simulated calcium occupancy P of the selectivity filter *vs* Q_f (red solid line) for bath concentration [Ca]=80mM. Single-ion Z_1 and double-ion Z_2 neutralisation points are labelled. (b) Single-ion (unsplit) occupancy profile for Z_1 point. (c) Double-ion (split) occupancy profile for Z_2 point.

VI. Conclusions

The analytic result (10) is found to agree with Brownian dynamics simulations, thus putatively accounting for how the position of the resonant point M_0^{CB+LB} is influenced by the radius of the Glutamate/Aspartate ring in NaChBac channels and their mutants [18], [23], [24]. The splitting of the Ca^{2+} profile is found in reasonable quantitative agreement with the results of BD simulations [6]. The local binding/repulsion leads to corrections of about 20 k_BT and to an observable splitting of the Ca^{2+} occupancy profiles. These results are also applicable to artificial sub-nm pores [25].

Acknowledgments

The research was supported by the Engineering and Physical Sciences Research Council UK (grant No. EP/M015831). We are grateful to M. Di Ventra, R. S. Eisenberg, O. A. Fedorenko, C. Guardiani, S. K. Roberts, and A. Stefanovska for comments and useful discussions.

References

[1] M. Krems and M. Di Ventra, "Ionic Coulomb blockade in nanopores," *J. Phys. Condens. Matter*, vol. 25, p. 065101, 2013.

[2] I. K. Kaufman, P. V. E. McClintock, and R. S. Eisenberg, "Coulomb blockade model of permeation and selectivity in biological ion channels," *New J. Phys.*, vol. 17, no. 8, p. 083021, 2015.

[3] I. Kaufman, W. Gibby, D. Luchinsky, P. McClintock, and R. Eisenberg, "Coulomb blockade oscillations in biological ion channels," in *Proc. 23rd Intern. Conf. on Noise and Fluctuations (ICNF), Xian*. IEEE Conf. Proc., June 2015, p. doi: 10.1109/ICNF.2015.7288558.

[4] C. W. J. Beenakker, "Theory of Coulomb-blockade oscillations in the conductance of a quantum dot," *Phys. Rev. B*, vol. 44, no. 4, pp. 1646–1656, 1991.

[5] B. Corry, T. W. Allen, S. Kuyucak, and S. H. Chung, "Mechanisms of permeation and selectivity in calcium channels," *Biophys. J.*, vol. 80, no. 1, pp. 195–214, 2001.

[6] I. K. Kaufman, D. G. Luchinsky, R. Tindjong, P. V. E. McClintock, and R. S. Eisenberg, "Multi-ion conduction bands in a simple model of calcium ion channels," *Phys. Biol.*, vol. 10, no. 2, p. 026007, 2013.

[7] G. Eisenman and R. Horn, "Ionic selectivity revisited: the role of kinetic and equilibrium processes in ion permeation through channels," *J. Membrane Biol.*, vol. 76, no. 3, pp. 197–225, 1983.

[8] S. O. Yesylevskyy and V. N. Kharkyanen, "Barrier-less knock-on conduction in ion channels: peculiarity or general mechanism?" *Chem. Phys.*, vol. 312, pp. 127–133, 2005.

[9] W. Nonner, L. Catacuzzeno, and B. Eisenberg, "Binding and selectivity in l-type calcium channels: A mean spherical approximation," *Biophys. J.*, vol. 79, no. 4, pp. 1976–1992, 2000.

[10] J. Zhang, A. Kamenev, and B. I. Shklovskii, "Conductance of ion channels and nanopores with charged walls: A toy model," *Phys. Rev. Lett.*, vol. 95, no. 14, p. 148101, 2005.

[11] J. Giri, J. E. Fonseca, D. Boda, D. Henderson, and B. Eisenberg, "Self-organized models of selectivity in calcium channels," *Phys. Biol.*, vol. 8, no. 2, p. 026004, 2011.

[12] A. Kamenev, J. Zhang, A. I. Larkin, and B. I. Shklovskii, "Transport in one-dimensional Coulomb gases: From ion channels to nanopores," *Physica A*, vol. 359, no. 0, pp. 129–161, 2006.

[13] D. Boda, M. Valiskó, B. Eisenberg, W. Nonner, D. Henderson, and D. Gillespie, "Combined effect of pore radius and protein dielectric coefficient on the selectivity of a calcium channel," *Physi. Rev. Lett.*, vol. 98, no. 16, p. 168102, 2007.

[14] A. Malasics, D. Gillespie, W. Nonner, D. Henderson, B. Eisenberg, and D. Boda, "Protein structure and ionic selectivity in calcium channels: Selectivity filter size, not shape, matters," *Biochim. Biophys. Acta (BBA)-Biomembranes*, vol. 1788, no. 12, pp. 2471–2480, 2009.

[15] D. G. Luchinsky, R. Tindjong, P. V. E. McClintock, I. Kaufman, and R. S. Eisenberg, "On selectivity and gating of ionic channels," in *SPIE Fourth International Symposium on Fluctuations and Noise*. International Society for Optics and Photonics, 2007, pp. 66 020D–66 020D.

[16] I. K. Kaufman, D. G. Luchinsky, R. Tindjong, P. V. E. McClintock, and R. S. Eisenberg, "Energetics of discrete selectivity bands and mutation-induced transitions in the calcium-sodium ion channels family," *Phys. Rev. E*, vol. 88, no. 5, p. 052712, 2013.

[17] P. T. Ellinor, J. Yang, W. A. Sather, J.-F. Zhang, and R. W. Tsien, "Ca^{2+} channel selectivity at a single locus for high-affinity ca^{2+} interactions," *Neuron*, vol. 15, no. 5, pp. 1121–1132, 1995.

[18] C. E. Naylor, C. Bagnéris, P. G. DeCaen, A. Sula, A. Scaglione, D. E. Clapham, and B. A. Wallace, "Molecular basis of ion permeability in a voltage-gated sodium channel," *EMBO J.*, p. doi: 10.15252/embj.201593285, 2016.

[19] E. von Kitzing, "A novel model for saturation of ion conductivity in transmembrane channels," in *Membrane Proteins: Structures, Interactions and Models: Proc. 25th Jerusalem Symposium on Quantum Chemistry and Biochemistry, Jerusalem, May 18-21, 1992*, A. Pullman, J. Jortner, and B. Pullman, Eds. Dordrecht: Kluwer, 1992, pp. 297–314.

[20] V. N. Kharkyanen, S. O. Yesylevskyy, and N. M. Berezetskaya, "Approximation of super-ions for single-file diffusion of multiple ions through narrow pores," *Phys. Rev. E*, vol. 82, p. 051103, 2010.

[21] D. G. Luchinsky, R. Tindjong, I. K. Kaufman, P. V. E. McClintock, and R. S. Eisenberg, "Self-consistent analytic solution for the current and the access resistance in open ion channels," *Phys. Rev. E*, vol. 80, no. 2, p. 021925, 2009.

[22] I. K. Kaufman, R. Tindjong, D. G. Luchinsky, P. V. E. McClintock, and R. S. Eisenberg, "Resonant multi-ion conduction in a simple model of calcium channels," in *22nd Intern. Conf. on Noise and Fluctuations (ICNF),* Montpellier, 24–28 June 2013, J. M. Routoure, L. Varani, and F. Pascal, Eds. IEEE Conf. Proc., 2013, p. doi: 10.1109/ICNF.2013.6578926.

[23] I. K. Kaufman, O. A. Fedorenko, D. G. Luchinsky, W. A. T. Gibby, S. K. McClintock, and R. S. Eisenberg, "Ionic coulomb blockade and anomalous mole fraction effect in NaChBac bacterial ion channels," *arXiv preprint arXiv:1612.02744*, 2016.

[24] C. Guardiani, P. M. Rodger, O. A. Fedorenko, S. K. Roberts, and I. A. Khovanov, "Sodium binding sites and permeation mechanism in the NaChBac channel: A molecular dynamics study," *J. Chem. Theor. Comp.*, p. 10.1021/acs.jctc.6b01035, 2016.

[25] J. Feng, K. Liu, M. Graf, D. Dumcenco, A. Kis, M. Di Ventra, and A. Radenovic, "Observation of ionic Coulomb blockade in nanopores," *Nature Mater.*, vol. 15, no. 8, pp. 850 – 855, 2016.